A Direct-Path Interference Resistant Passive Detector

Xin Zhang, Hongbin Li, *Senior Member, IEEE*, and Braham Himed, *Fellow, IEEE*

***Abstract*—Passive radar, which detects and tracks targets of interest by using noncooperative illuminators of opportunity (IOs), has become popular since qualified IO sources are widely accessible nowadays. This letter examines the target detection problem for a passive multistatic radar, where the receivers are contaminated by nonnegligible noise and direct-path interference (DPI). The signal transmitted from the IO is treated as a deterministic but unknown process. A generalized likelihood ratio test approach is proposed, where the $\mathcal{H}_1$ estimation problem is solved using an iterative method. A clairvoyant matched filtering detector, which assumes the knowledge of the IO waveform, is provided as well to benchmark performance. Simulation results are presented to show the effectiveness of the proposed detector in the presence of DPI.**

***Index Terms*—Direct-path interference (DPI), generalized likelihood ratio test (GLRT), passive multistatic detection.**

I. Introduction

PASSIVE radar exploits noncooperative illuminators of opportunity (IOs), such as television, radio, and cellular signals, to detect and track objects of interest [1]–[4]. Using existing ambient signals, passive radar can easily be deployed without incurring additional spectrum usage. Furthermore, passive radar can readily employ a multistatic configuration by leveraging multiple IOs at different locations, which will lead to spatial diversity and improved performance [5], [6].

However, passive sensing is more challenging than its active counterpart because the IO waveform is unknown to the receivers. To deal with this difficulty, one popular solution is to employ a reference channel (RC) at the receiver to collect the direct-path (transmitter-to-receiver) signal and, as well, a separate surveillance channel (SC) to collect the target echo [1], [2], [4]. Then, a cross-correlation (CC) operation is conducted between the RC and SC, which resembles the matched filtering (MF) approach used in active radar. It should be pointed out that, due to the presence of noise in the RC, the CC is suboptimal and has been shown to be highly sensitive to the RC noise [7]. Recently, new improved passive detectors were introduced by taking into account the effect of noisy RC [8], [9]. IO waveform estimation with noisy RC and the prior knowledge that the waveform resides in a low-dimensional subspace is examined in [10]. Aside from the above studies, where the IO waveform is treated as a deterministic process, another approach to deal with the unknown IO waveform is to model it as a stochastic process. One simple way is to treat the samples of the waveform as independent and identically distributed Gaussian variables. Two stochastic passive detectors were derived based on this idea in [9]. However, the IO waveform is in general correlated due to coding, modulation, pulse shaping, and other transmitter processing. Stemming from this fact, [11] considered the problem of estimating the delay and Doppler frequency of a target signal in passive sensing by modeling the IO waveform as a correlated Gaussian process. In [12], the authors studied the delay-Doppler estimation problem in passive radar using orthogonal frequency-division multiplexing (OFDM) communication IO sources. Meanwhile, a number of studies considered passive detection with multichannel observations obtained via, e.g., multiple spatially distributed sensors [13]–[15], where the interchannel correlation of the observations can be exploited, which circumvents the need for a separate RC.

The handling of direct-path interference (DPI), i.e., the direct transmission from the IO source to the SC, is another major challenge in passive radar. The DPI is generally significantly stronger (by many tens to even over a hundred dB) than the target echo [16]. In [7], it was shown that a modest level of DPI can significantly degrade the performance of the CC detector. Therefore, passive radar has to employ some interference cancellation technique, such as an adaptive antenna with a null formed in the direction of the IO, and/or a temporal filter that utilizes the reference signal in the RC to cancel the DPI [17]. Despite such cancellation, some residual DPI may still exist due to, e.g., limited array size and null depth [18]. As a result, the DPI may still be at a nonnegligible power level compared with the target echo. However, most existing work on passive detection, e.g., [1], [2], [8], [9], [13]–[15], did not account for the residual DPI.

In this letter, we examine target detection for a passive multistatic radar system, where the receivers are contaminated by nonnegligible noise and DPI. We propose an iterative approach that models the unknown IO waveform as a deterministic process. The solution is developed under the generalized likelihood ratio test (GLRT) framework. Our proposed detector is an extension of the algorithm proposed in [14], by taking into account the DPI effect. For performance benchmarking, a clairvoyant MF detector that assumes the exact knowledge of the IO waveform is also developed. Numerical results show that the proposed

Manuscript received December 14, 2016; revised February 21, 2017; accepted March 23, 2017. Date of publication March 28, 2017; date of current version April 28, 2017. This work was supported in part by a subcontract with Matrix Research, Inc., for research sponsored by the Air Force Research Laboratory and in part by the National Science Foundation under Grant ECCS-1609393. The associate editor coordinating the review of this manuscript and approving it for publication was Dr. Martin Ulmke. *(Corresponding author: Hongbin Li.)*

X. Zhang and H. Li are with the Department of Electrical and Computer Engineering, Stevens Institute of Technology, Hoboken, NJ 07030 USA (e-mail: xzhang23@stevens.edu; Hongbin.Li@stevens.edu).

B. Himed is with the AFRL/RYMD, Dayton, OH 45433 USA (e-mail: braham.himed@us.af.mil).

Color versions of one or more of the figures in this letter are available online at http://ieeexplore.ieee.org.

Digital Object Identifier 10.1109/LSP.2017.2688459

1070-9908 © 2017 IEEE. Personal use is permitted, but republication/redistribution requires IEEE permission.
See http://www.ieee.org/publications_standards/publications/rights/index.html for more information.

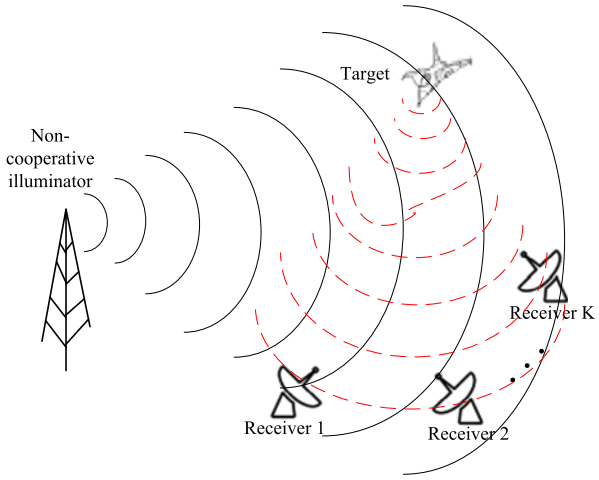

Fig. 1. Configuration of a multistatic passive radar system (dashed red line represents the reflection from the target).

passive multistatic detector significantly outperforms the detector in [14], especially when the DPI is strong.

II. Problem Formulation

Consider a multistatic passive radar system, as shown in Fig. 1, which contains one noncooperative IO and K distributed receivers. The signal collected by the kth receiver (channel) in the presence of a target, denoted by $y_k'(t)$, can be expressed as

$$y_k'(t) = \beta_k x(t-d_k) + \alpha_k' x(t-t_k)\, e^{\jmath 2\pi f_k t} + n_k'(t) \qquad k = 1, 2, \ldots, K \quad (1)$$

where $x(t)$ is the unknown signal (baseband equivalent) transmitted by the IO, d_k is the propagation delay from the IO to the kth receiver, i.e., the propagation delay of the DPI, t_k is the propagation delay of the target, due to the transmission from the IO to the target and then from the target to the kth receiver, f_k is the target's Doppler frequency seen at the kth receiver, β_k is the scaling coefficient that includes the antenna attenuation and the channel propagation effects from the IO to the kth receiver, α_k' is the scaling coefficient accounting for the target reflectivity, the antenna gain, and the channel propagation effects, and $n_k'(t)$ is the additive zero-mean white Gaussian noise at the kth channel with power (variance) η.

To simplify the system model, we observe that the direct-path delay d_k is generally known *a priori* and can be compensated for, since the location of the IO is usually known to each receiver. Let $y_k(t) = y_k'(t+d_k)$ denote the kth delay-compensated signal, and the delay-compensated noise $n_k(t)$ is similarly defined. This leads to

$$y_k(t) = \beta_k x(t) + \alpha_k x(t-\tau_k) e^{\jmath 2\pi f_k t} + n_k(t) \quad (2)$$

where τ_k is the kth bistatic delay given by $\tau_k = t_k - d_k$ and $\alpha_k = \alpha_k' e^{\jmath 2\pi f_k d_k}$.

We assume that $x(t)$ has a duration of T s, e.g., due to the framed transmissions employed by the IO, in which case T represents the frame duration. The observation interval T_o is selected such that $T_o \geq T + \tau_{\max}$, where $\tau_{\max}$ denotes the maximum bistatic delay that can be tolerated by the system. We sample each channel using a sampling frequency $f_s \geq 2(B + f_{\max})$, where B denotes the bandwidth of the signal $x(t)$ and $f_{\max}$ is the maximum Doppler frequency of the target that is designed detectable by the system. Suppose M samples are collected for each channel over the observation window T_o, i.e., $T_o = MT_s$, where $T_s = 1/f_s$ denotes the sampling interval. Let $\mathbf{y}_k$, $\mathbf{x}$, and $\mathbf{n}_k$ be $M \times 1$ vectors formed by M adjacent samples of $y_k(t)$, $x(t)$, and $n_k(t)$, respectively. In addition, the M-point discrete Fourier transform matrix $\mathbf{T}$ has entries $[\mathbf{T}]_{p,q} = e^{-\jmath 2\pi (p-1)\Delta f (q-1) T_s}/\sqrt{M}$, $p, q = 1, 2, \ldots, M$, with the frequency domain sampling spacing $\Delta f = \frac{f_s}{M} = \frac{1}{T_s M}$, and $\mathbf{W}(x)$ is a diagonal matrix with diagonal entries $[\mathbf{W}(x)]_{p,p} = e^{\jmath 2\pi (p-1)x}$, $p = 1, 2, \ldots, M$. The discretized model can be written as [11], [13]

$$\mathbf{y}_k = \beta_k \mathbf{x} + \alpha_k \mathcal{D}(\tau_k, f_k)\mathbf{x} + \mathbf{n}_k,\ k = 1, 2, \ldots, K \quad (3)$$

where the channel noise $\mathbf{n}_k$ is a zero-mean white Gaussian noise with covariance matrix $\eta \mathbf{I}_M$ and

$$\mathcal{D}(\tau_k, f_k) = \mathbf{W}(f_k T_s)\mathbf{T}^H \mathbf{W}(-\tau_k \Delta f)\mathbf{T}. \quad (4)$$

The problem of interest is to determine if a target is present in the cell of interest (test cell) using the observations $\{\mathbf{y}_k\}$. For each cell under test, the detection problem can be described by the following composite binary hypothesis test [8], [9], [13], [14], [19]:

$$\begin{aligned} \mathcal{H}_1 : \mathbf{y}_k &= \beta_k \mathbf{x} + \alpha_k \mathcal{D}(\tau_k, f_k)\mathbf{x} + \mathbf{n}_k \\ \mathcal{H}_0 : \mathbf{y}_k &= \beta_k \mathbf{x} + \mathbf{n}_k \\ & \qquad k = 1, 2, \ldots, K \end{aligned} \quad (5)$$

where the unknowns are the IO waveform $\mathbf{x}$, $\boldsymbol{\beta} = [\beta_1, \beta_2, \ldots, \beta_K]^T$, $\boldsymbol{\alpha} = [\alpha_1, \alpha_2, \ldots, \alpha_K]^T$, and the channel noise power η. Note that the data model has a multiplicative ambiguity among α_k, β_k, and $\mathbf{x}$, which makes these parameters not uniquely identifiable. To resolve the ambiguity, we impose an additional constraint $\|\mathbf{x}\| = 1$. This constraint does not have any impact on the detection problem.

In radar detection, it is customary to divide the uncertainty region of the target delay and Doppler frequency into small cells and each cell is tested for the presence or absence of a target [20]. Therefore, for each cell under test, $\mathcal{D}(\tau_k, f_k)$ is known because the delay and Doppler associated with that cell is known. For notational simplicity, we henceforth use $\mathcal{D}_k$ for $\mathcal{D}(\tau_k, f_k)$.

III. Proposed Detectors

In this section, we develop a detector for the problem (5) under the GLRT framework. In addition, a clairvoyant MF detector is derived, assuming that the IO waveform is known, and can be used to benchmark the detection performance in the presence of DPI.

A. GLRT Detector

The GLRT principle requires the maximum likelihood estimates (MLEs) of the unknown parameters under both hypotheses. Let the observations from K receivers be stacked as

$\mathbf{Y} = [\mathbf{y}_1, \mathbf{y}_2, \ldots, \mathbf{y}_K]$. Then, the GLRT is given by

$$\frac{\max_{\{\boldsymbol{\alpha},\boldsymbol{\beta},\mathbf{x},\eta\}} p(\mathbf{Y}|\boldsymbol{\alpha},\boldsymbol{\beta},\mathbf{x},\eta)}{\max_{\{\boldsymbol{\beta},\mathbf{x},\eta\}} p(\mathbf{Y}|\boldsymbol{\beta},\mathbf{x},\eta)} \underset{\mathcal{H}_0}{\overset{\mathcal{H}_1}{\gtrless}} \zeta \tag{6}$$

where $p(\mathbf{Y}|\boldsymbol{\alpha},\boldsymbol{\beta},\mathbf{x},\eta)$ and $p(\mathbf{Y}|\boldsymbol{\beta},\mathbf{x},\eta)$ denote the likelihood functions under $\mathcal{H}_1$ and $\mathcal{H}_0$, respectively. In the following, we present the solutions to the two maximum likelihood estimation problems in (6), and the estimates are used in the GLRT detector.

Under $\mathcal{H}_1$, the likelihood function can be written as

$$p(\mathbf{Y}|\boldsymbol{\alpha},\boldsymbol{\beta},\mathbf{x},\eta) = \frac{1}{(\pi\eta)^{KM}} \exp\left\{-\frac{1}{\eta}\sum_{k=1}^{K} \|\mathbf{y}_k - \beta_k\mathbf{x} - \alpha_k\mathcal{D}_k\mathbf{x}\|^2\right\}. \tag{7}$$

The MLEs of $\{\boldsymbol{\alpha},\boldsymbol{\beta}\}$, as functions of the IO waveform $\mathbf{x}$, can be written as

$$\left[\hat{\alpha}_k, \hat{\beta}_k\right]^T = \left(\mathbf{H}_k^H\mathbf{H}_k\right)^{-1}\mathbf{H}_k^H\mathbf{y}_k \tag{8}$$

where $\mathbf{H}_k = [\mathcal{D}_k\mathbf{x}, \mathbf{x}]$. Substituting the above estimates back into the likelihood function, we have

$$\hat{\mathbf{x}} = \arg\min_{\|\mathbf{x}\|=1} \sum_{k=1}^{K} \left\|\mathbf{P}_k^{\perp}\mathbf{y}_k\right\|^2 = \arg\max_{\|\mathbf{x}\|=1} \sum_{k=1}^{K} \mathbf{y}_k^H\mathbf{P}_k\mathbf{y}_k \tag{9}$$

where the projection matrices are given by $\mathbf{P}_k^{\perp} = \mathbf{I} - \mathbf{P}_k$ and $\mathbf{P}_k = \mathbf{H}_k\left(\mathbf{H}_k^H\mathbf{H}_k\right)^{-1}\mathbf{H}_k^H$. Expanding further the objective function, we obtain

$$\begin{aligned}
&\sum_{k=1}^{K} \mathbf{y}_k^H\mathbf{P}_k\mathbf{y}_k \\
&= \sum_{k=1}^{K} \mathbf{y}_k^H\mathbf{H}_k\left(\mathbf{H}_k^H\mathbf{H}_k\right)^{-1}\mathbf{H}_k^H\mathbf{y}_k \\
&= \sum_{k=1}^{K} \left[\mathbf{y}_k^H\mathcal{D}_k\mathbf{x}, \mathbf{y}_k^H\mathbf{x}\right] \begin{bmatrix} \|\mathbf{x}\|^2 & \mathbf{x}^H\mathcal{D}_k^H\mathbf{x} \\ \mathbf{x}^H\mathcal{D}_k\mathbf{x} & \|\mathbf{x}\|^2 \end{bmatrix}^{-1} \\
&\times \begin{bmatrix} \mathbf{x}^H\mathcal{D}_k^H\mathbf{y}_k \\ \mathbf{x}^H\mathbf{y}_k \end{bmatrix} \\
&= \sum_{k=1}^{K} \frac{1}{\|\mathbf{x}\|^4 - |\mathbf{x}^H\mathcal{D}_k\mathbf{x}|^2}\big(\|\mathbf{x}\|^2\mathbf{x}^H\mathcal{D}_k^H\mathbf{y}_k\mathbf{y}_k^H\mathcal{D}_k\mathbf{x} \\
&+ \|\mathbf{x}\|^2\mathbf{x}^H\mathbf{y}_k\mathbf{y}_k^H\mathbf{x} - \mathbf{x}^H\mathcal{D}_k\mathbf{x}\mathbf{x}^H\mathcal{D}_k^H\mathbf{y}_k\mathbf{y}_k^H\mathbf{x} \\
&- \mathbf{x}^H\mathcal{D}_k^H\mathbf{x}\mathbf{x}^H\mathbf{y}_k\mathbf{y}_k^H\mathcal{D}_k\mathbf{x}\big) \\
&= \mathbf{x}^H\boldsymbol{\Theta}(\mathbf{x})\mathbf{x}
\end{aligned} \tag{10}$$

where

$$\begin{aligned}
\boldsymbol{\Theta}(\mathbf{x}) = \sum_{k=1}^{K} \big(&\omega_{1,k}(\mathbf{x})\mathcal{D}_k^H\mathbf{y}_k\mathbf{y}_k^H\mathcal{D}_k + \omega_{1,k}(\mathbf{x})\mathbf{y}_k\mathbf{y}_k^H \\
&+ \omega_{2,k}^*(\mathbf{x})\mathcal{D}_k^H\mathbf{y}_k\mathbf{y}_k^H + \omega_{2,k}(\mathbf{x})\mathbf{y}_k\mathbf{y}_k^H\mathcal{D}_k\big)
\end{aligned} \tag{11}$$

and

$$\omega_{1,k}(\mathbf{x}) = \frac{\|\mathbf{x}\|^2}{\|\mathbf{x}\|^4 - |\mathbf{x}^H\mathcal{D}_k\mathbf{x}|^2} = \frac{1}{1 - |\mathbf{x}^H\mathcal{D}_k\mathbf{x}|^2} \tag{12}$$

Algorithm 1: Proposed Approach.

Initialization: $l = 0$ and $\mathbf{x}^{(0)} = \sum_{k=1}^{K}\mathbf{y}_k / \|\sum_{k=1}^{K}\mathbf{y}_k\|$.
for $l = 0, 1, 2, \ldots$ **do**
1) Compute $\boldsymbol{\Theta}^{(l)}$ by substituting $\mathbf{x}^{(l)}$ into $\boldsymbol{\Theta}(\mathbf{x})$.
2) $\mathbf{x}^{(l+1)} = \arg\max_{\|\mathbf{x}\|=1} \mathbf{x}^H\boldsymbol{\Theta}^{(l)}\mathbf{x}$, i.e., the principal eigenvector of $\boldsymbol{\Theta}^{(l)}$, and $\gamma^{(l+1)}$ is the corresponding principal eigenvalue.
3) Check convergence.
end for

$$\omega_{2,k}(\mathbf{x}) = \frac{-\mathbf{x}^H\mathcal{D}_k^H\mathbf{x}}{\|\mathbf{x}\|^4 - |\mathbf{x}^H\mathcal{D}_k\mathbf{x}|^2} = \frac{-\mathbf{x}^H\mathcal{D}_k^H\mathbf{x}}{1 - |\mathbf{x}^H\mathcal{D}_k\mathbf{x}|^2}. \tag{13}$$

If the dependence of $\boldsymbol{\Theta}(\mathbf{x})$ on $\mathbf{x}$ is neglected, the right-hand side of (10) is a quadratic form with respect to $\mathbf{x}$, which is maximized by the principal eigenvector of $\boldsymbol{\Theta}$. Therefore, we propose an iterative approach to maximize (10), where the current iteration fixes the matrix $\boldsymbol{\Theta}(\mathbf{x})$ by using the estimated $\mathbf{x}$ from the previous iteration and then maximizes the resulted quadratic form. Similar iterative approaches were also utilized in [21]–[24] for radar waveform design. The proposed iterative approach is summarized in Algorithm 1.

Let γ be the final update of the principal eigenvalue after all iterations. The noise power can be estimated as

$$\hat{\eta}_1 = \frac{\sum_{k=1}^{K}\|\mathbf{y}_k\|^2 - \gamma}{MK}. \tag{14}$$

Under $\mathcal{H}_0$, the received data is free of target echoes, and the unknown parameters are $\{\boldsymbol{\beta}, \eta, \mathbf{x}\}$. The likelihood function is similar to (7) with $\boldsymbol{\alpha} = \mathbf{0}$. The MLE of β_k can be written as

$$\hat{\beta}_k = \left(\mathbf{x}^H\mathbf{x}\right)^{-1}\mathbf{x}^H\mathbf{y}_k. \tag{15}$$

Inserting (15) into the likelihood function, we obtain

$$\hat{\mathbf{x}} = \arg\max_{\|\mathbf{x}\|=1} \mathbf{x}^H\mathbf{Y}\mathbf{Y}^H\mathbf{x} \tag{16}$$

which is the principal eigenvector of the matrix $\mathbf{Y}\mathbf{Y}^H$. Finally, the MLE of the noise power is obtained as [14]

$$\hat{\eta}_0 = \frac{\sum_{k=1}^{K}\|\mathbf{y}_k\|^2 - \lambda_1}{MK} \tag{17}$$

where λ_1 denotes the largest eigenvalue of $\boldsymbol{\Phi} \triangleq \mathbf{Y}^H\mathbf{Y}$.

By applying the above results to (6) followed by simplification, the GLRT detector is given by

$$\frac{\sum_{k=1}^{K}\|\mathbf{y}_k\|^2 - \lambda_1}{\sum_{k=1}^{K}\|\mathbf{y}_k\|^2 - \gamma} \underset{\mathcal{H}_0}{\overset{\mathcal{H}_1}{\gtrless}} \xi \tag{18}$$

where ξ is a suitably modified version of the threshold in (6). Denote $\lambda_1 \geq \lambda_2 \geq \ldots \geq \lambda_K$ as the ordered eigenvalues of the K-dimensional matrix $\boldsymbol{\Phi}$. To gain an insight into the structure of the proposed GLRT detector, we equivalently write (18) as

$$\frac{1}{\frac{1}{MK}\sum_{k=2}^{K}\lambda_k}\left(\gamma - \lambda_1\right) \underset{\mathcal{H}_0}{\overset{\mathcal{H}_1}{\gtrless}} \bar{\xi} \tag{19}$$

where the result $\sum_{k=1}^{K}\|\mathbf{y}_k\|^2 = \mathrm{tr}\{\boldsymbol{\Phi}\} = \sum_{k=1}^{K}\lambda_k$ is utilized and $\bar{\xi} = MK(1 - 1/\xi)$. We notice that the denominator in (19)

is exactly the MLE of the noise power under $\mathcal{H}_0$. Therefore, the test statistic in (19) is the difference between the two principal eigenvalues normalized by the estimated noise power.

B. Clairvoyant MF Detector

For comparison, we derive a clairvoyant MF detector in the presence of DPI under the GLRT framework. The detector is clairvoyant because it assumes that the IO waveform is known. It serves as a benchmark for passive detection with DPI.

Under $\mathcal{H}_1$ and starting from the likelihood function (7) but with $\mathbf{x}$ known, we obtain the same expressions as in (8) for the estimates of $\{\boldsymbol{\alpha}, \boldsymbol{\beta}\}$. Then, the estimate of the noise power is given by

$$\hat{\eta}_{\text{MF},1} = \frac{1}{MK}\left(\sum_{k=1}^{K}\|\mathbf{y}_k\|^2 - \sum_{k=1}^{K}\mathbf{y}_k^H\mathbf{P}_k\mathbf{y}_k\right) \tag{20}$$

where the projection matrices $\{\mathbf{P}_k\}$ are known in the current case. Under $\mathcal{H}_0$, the MLE of the noise power is

$$\hat{\eta}_{\text{MF},0} = \frac{1}{MK}\left(\sum_{k=1}^{K}\|\mathbf{y}_k\|^2 - \frac{\mathbf{x}^H\mathbf{Y}\mathbf{Y}^H\mathbf{x}}{\mathbf{x}^H\mathbf{x}}\right). \tag{21}$$

Consequently, the clairvoyant MF detector can be written as

$$\mathcal{L}_{\text{MF}} = \frac{1}{\hat{\eta}_{\text{MF},1}}\hat{\eta}_{\text{MF},0}. \tag{22}$$

IV. Numerical Simulations

In this section, numerical results are presented to illustrate the performance of the proposed detectors. The algorithm proposed in [14] is included in our comparison, which is referred to as the LAM detector since its test variable is the ratio between the largest eigenvalue and the arithmetic mean of eigenvalues, i.e., $K\lambda_1/\sum_{k=1}^{K}\lambda_k$. Note that the LAM detector neglects the DPI. For fairness, we also include in comparison a modified generalized canonical correlation (mGCC) detector, which extends the original GCC detector [19] with DPI cancellation. Specifically, the mGCC first estimates the IO waveform as the principal eigenvector of the sample covariance matrix $\mathbf{Y}\mathbf{Y}^H$ [13], [14], which is then used to form an estimate of the DPI that is subsequently subtracted from the observation. The residual is then input into the GCC detector for target detection. In the following, the signal-to-noise ratio (SNR) is defined as $\sum_{k=1}^{K}|\alpha_k|^2/K\eta$, and the DPI-to-noise ratio (DNR) as $\sum_{k=1}^{K}|\beta_k|^2/K\eta$.

The detection probability curves versus SNR are plotted in Fig. 2, where the observation length $M = 20$ and channel number $K = 3$. Two cases of different DNRs are considered. In the first case when DNR $= 0$ dB, i.e., moderate DPI, the proposed detector is slightly better than the LAM detector, whereas the mGCC detector is almost the same as the proposed one. When the DNR increases to 20 dB, i.e., strong DPI, the proposed detector and the mGCC become significantly better than the LAM detector, thanks to their ability to handle the DPI. In addition, it can be seen that the proposed method is closer to the MF and better than the mGCC. This is because the proposed method can benefit more from a strong direct path signal.

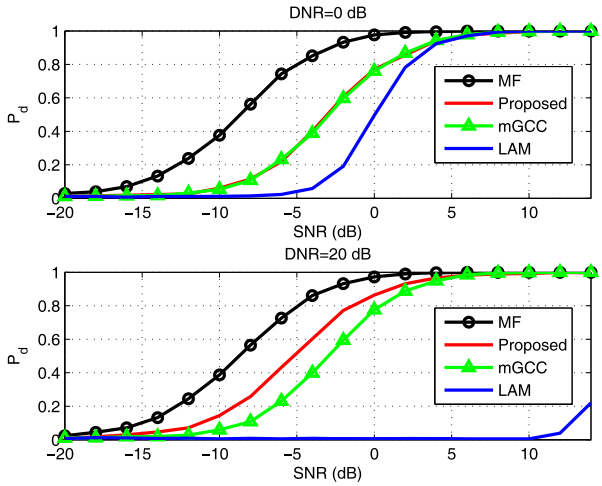

Fig. 2. Detection performance versus SNR with $M = 20$, $K = 3$.

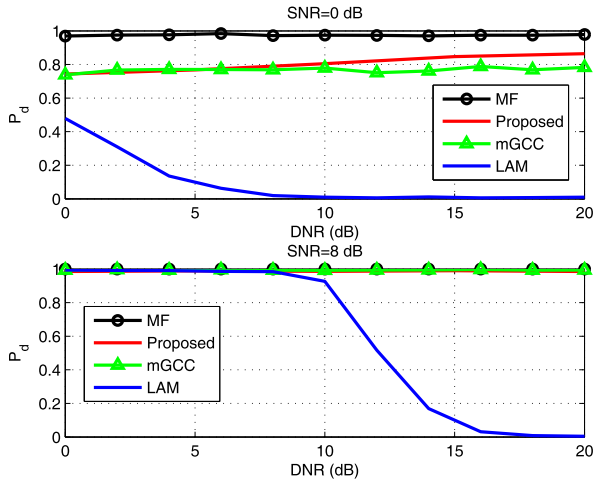

Fig. 3. Detection performance versus DNR with $M = 20$, $K = 3$.

Fig. 3 illustrates the detection performance versus DNR. We can see that the proposed and the mGCC detectors significantly outperform the LAM detector, especially in the high DNR region. When SNR $= 0$ dB, it is seen that the proposed detector improves as DNR increases while the mGCC exhibits little changes, which indicates that the proposed method can not only mitigate the DPI but also exploit it for passive detection.

V. Conclusion

In this letter, we considered the target detection problem for a multistatic passive radar system by taking the DPI into account. We proposed a GLRT detector by treating the unknown IO waveform as a deterministic process and utilizing an iterative method for estimation. We also proposed a clairvoyant MF method which, along with the conventional LAM detector and the modified GCC detector, is included in performance comparison. Numerical results show that the proposed detector performs better than the mGCC detector and significantly outperforms the LAM detector that ignores the DPI.

REFERENCES

[1] H. D. Griffiths and C. J. Baker, "Passive coherent location radar systems. Part 1: performance prediction," *IEE Proc. Radar, Sonar Navigat.*, vol. 152, no. 3, pp. 124–132, Jun. 2005.

[2] P. E. Howland, D. Maksimiuk, and G. Reitsma, "FM radio based bistatic radar," *IEE Proc. Radar, Sonar Navigat.*, vol. 152, no. 3, pp. 107–115, Jun. 2005.

[3] S. Gogineni, M. Rangaswamy, B. D. Rigling, and A. Nehorai, "Ambiguity function analysis for UMTS-based passive multistatic radar," *IEEE Trans. Signal Process.*, vol. 62, no. 11, pp. 2945–2957, Jun. 2014.

[4] T. Shan, S. Liu, Y. D. Zhang, M. G. Amin, R. Tao, and Y. Feng, "Efficient architecture and hardware implementation of coherent integration processor for digital video broadcast-based passive bistatic radar," *IET Radar, Sonar Navigat.*, vol. 10, no. 1, pp. 97–106, Jan. 2016.

[5] Q. He and R. S. Blum, "The significant gains from optimally processed multiple signals of opportunity and multiple receive stations in passive radar," *IEEE Signal Process. Lett.*, vol. 21, no. 2, pp. 180–184, Feb. 2014.

[6] Q. He, J. Hu, R. S. Blum, and Y. Wu, "Generalized Cramér-Rao bound for joint estimation of target position and velocity for active and passive radar networks," *IEEE Trans. Signal Process.*, vol. 64, no. 8, pp. 2078–2089, April 2016.

[7] J. Liu, H. Li, and B. Himed, "On the performance of the cross-correlation detector for passive radar applications," *Signal Process.*, vol. 113, pp. 32–37, 2015.

[8] D. E. Hack, L. K. Patton, B. Himed, and M. A. Saville, "Detection in passive MIMO radar networks," *IEEE Trans. Signal Process.*, vol. 62, no. 11, pp. 2999–3012, Jun. 2014.

[9] G. Cui, J. Liu, H. Li, and B. Himed, "Signal detection with noisy reference for passive sensing," *Signal Process.*, vol. 108, pp. 389–399, Mar. 2015.

[10] P. Setlur, S. Gogineni, and M. Rangaswamy, "Waveform extraction from reference channels of passive multistatic radar systems," in *Proc. 49th Asilomar Conf. Signals, Syst. Comput.*, Pacific Grove, CA, USA, Nov. 2015, pp. 1696–1701.

[11] X. Zhang, H. Li, J. Liu, and B. Himed, "Joint delay and Doppler estimation for passive sensing with direct-path interference," *IEEE Trans. Signal Process.*, vol. 64, no. 3, pp. 630–640, Feb. 2016.

[12] L. Zheng and X. Wang, "Super-resolution delay-Doppler estimation for OFDM passive radar," *IEEE Trans. Signal Process.*, vol. 65, no. 9, pp. 2197–2210, May 2017.

[13] D. E. Hack, L. K. Patton, B. Himed, and M. A. Saville, "Centralized passive MIMO radar detection without direct-path reference signals," *IEEE Trans. Signal Proc.*, vol. 62, no. 11, pp. 3013–3023, Jun. 2014.

[14] J. Liu, H. Li, and B. Himed, "Two target detection algorithms for passive multistatic radar," *IEEE Trans. Signal Proc.*, vol. 62, no. 22, pp. 5930–5939, Nov. 2014.

[15] D. E. Hack, C. W. Rossler, and L. K. Patton, "Multichannel detection of an unknown rank-N signal using uncalibrated receivers," *IEEE Signal Process. Lett.*, vol. 21, no. 8, pp. 998–1002, May 2014.

[16] O. Rabaste and D. Poullin, "Rejection of Doppler shifted multipaths in airborne passive radar," in *Proc. 2015 IEEE Int. Radar Conf.*, Arlington, VA, USA, May 2015, pp. 1660–1665.

[17] Y. Ma, T. Shan, Y. D. Zhang, M. G. Amin, R. Tao, and Y. Feng, "A novel two-dimensional sparse-weight NLMS filtering scheme for passive bistatic radar," *IEEE Geosci. Remote Sens. Lett.*, vol. 13, no. 5, pp. 676–680, May 2016.

[18] R. Tao, H. Z. Wu, and T. Shan, "Direct-path suppression by spatial filtering in digital television terrestrial broadcasting-based passive radar," *IET Radar, Sonar Navigat.*, vol. 4, no. 6, pp. 791–805, Dec. 2010.

[19] K. S. Bialkowski, I. V. L. Clarkson, and S. D. Howard, "Generalized canonical correlation for passive multistatic radar detection," in *Proc. 2011 IEEE Statist. Signal Process. Workshop*, Jun. 2011, pp. 417–420.

[20] M. A. Richards, *Fundamentals of Radar Signal Processing*. New York, NY, USA: McGraw-Hill, 2005.

[21] S. U. Pillai, H. S. Oh, D. C. Youla, and J. R. Guerci, "Optimal transmit-receiver design in the presence of signal-dependent interference and channel noise," *IEEE Trans. Inf. Theory*, vol. 46, no. 2, pp. 577–584, Mar. 2000.

[22] B. Friedlander, "Waveform design for MIMO radars," *IEEE Trans. Aerosp. Electron. Syst.*, vol. 43, no. 3, pp. 1227–1238, Jul. 2007.

[23] C. Y. Chen and P. P. Vaidyanathan, "MIMO radar waveform optimization with prior information of the extended target and clutter," *IEEE Trans. Signal Process.*, vol. 57, no. 9, pp. 3533–3544, Sep. 2009.

[24] G. Cui, H. Li, and M. Rangaswamy, "MIMO radar waveform design with constant modulus and similarity constraints," *IEEE Trans. Signal Process.*, vol. 62, no. 2, pp. 343–353, Jan. 2014.